

## Electronic Supplementary Information

### **Cobalt phosphide nanorings towards efficient electrocatalytic nitrate reduction to ammonia†**

Qing-Ling Hong<sup>a</sup>, Jia Zhou<sup>a</sup>, Quan-Guo Zhai<sup>a</sup>, Yu-Cheng Jiang<sup>a</sup>, Man-Cheng Hu<sup>a</sup>, Xue Xiao<sup>b\*</sup>, Shu-Ni Li<sup>a\*</sup>, and Yu Chen<sup>c</sup>

<sup>a</sup> *Key Laboratory of Macromolecular Science of Shaanxi Province, School of Chemistry and Chemical Engineering, Shaanxi Normal University, Xi'an 710062, PR China. China. E-mail: lishuni@snnu.edu.cn (S. Li)*

<sup>b</sup> *Centre for Translational Atomaterials, School of Science, Computing and Engineering Technologies, Swinburne University of Technology, Hawthorn, VIC 3122, Australia. E-mail: tiffanyxx110@gmail.com (X. Xiao)*

<sup>c</sup> *School of Materials Science and Engineering, Shaanxi Normal University, Xi'an 710062, PR China.*

## Experimental section

### Reagents and chemicals

Cobalt (II) chloride hexahydrate ( $\text{CoCl}_2 \cdot 6\text{H}_2\text{O}$ ), sodium hydroxide (NaOH, 97%), hydrogen peroxide ( $\text{H}_2\text{O}_2$ , 30%), sodium sulfate ( $\text{Na}_2\text{SO}_4$ , 99%), sodium hypophosphite monohydrate ( $\text{NaH}_2\text{PO}_2 \cdot \text{H}_2\text{O}$ , 99%), and sodium nitrate ( $\text{NaNO}_3$ , 99%) were purchased from Sinopharm Chemical Reagent Co., Ltd. (Shanghai, People's Republic of China). All reagents in this work are analytically pure and can be used directly without further purification.

### Synthesis of CoOOH NRs

In a typical synthesis, 3 mL of NaOH (0.15 M) solution was added into 20 mL of  $\text{CoCl}_2$  (0.2 mM) solution and stirred for 10 min, which generate  $\text{Co}(\text{OH})_2$  nanosheets ( $\text{Co}(\text{OH})_2$  NSs). Then, 40  $\mu\text{L}$  of  $\text{H}_2\text{O}_2$  (30%) solution was added in above  $\text{Co}(\text{OH})_2$  NSs suspension. After stirring for 3 hours at 60°C, CoOOH nanorings (CoOOH NRs) were collected by centrifugation, and then dried in vacuum at 60 °C for 5 hours.

### Synthesis of CoP NRs

CoP nanorings (CoP NRs) were prepared by high-temperature phosphating of CoOOH NRs in the presence of  $\text{NaH}_2\text{PO}_2 \cdot \text{H}_2\text{O}$ . Specifically, 20 mg of CoOOH NRs and 200 mg of  $\text{NaH}_2\text{PO}_2 \cdot \text{H}_2\text{O}$  were mixed uniformly into a porcelain boat. The quartz tube was heated at 300 °C for 30 min with a heating rate of 1°C min<sup>-1</sup> under N<sub>2</sub> atmosphere. After reaction, CoP NRs were washed by water and dried in vacuum at 60 °C.

### Synthesis of CoP NPs

In a typical synthesis, 20 mg of  $\text{Co}(\text{OH})_2$  NSs and 200 mg of  $\text{NaH}_2\text{PO}_2 \cdot \text{H}_2\text{O}$  were mixed uniformly into a porcelain boat. The quartz tube was heated at 300 °C for 30 min with a heating rate of 1°C min<sup>-1</sup> under N<sub>2</sub> atmosphere. After reaction, CoP NPs were washed by water and dried in vacuum at 60 °C.

### Physical characterization

The morphology and composition of the samples were characterized by SU-8020 scanning electron microscopy (SEM) equipped with energy dispersive X-ray spectroscopy (EDX). Transmission electron microscope (TEM) image and selected

area electron diffraction (SAED) pattern were obtained at TECNAI G2 F20 instrument. A DX-2700 power X-ray diffractometer was used to achieve powder X-ray diffraction (PXRD) patterns. X-ray photoelectron spectroscopy (XPS) measurements were carried out on AXIS ULTRA spectrometer. The binding energy was corrected for specimen charging by referencing C 1s to 284.5 eV.

### **Characterization of Co(OH)<sub>2</sub> nanosheets (Co(OH)<sub>2</sub> NSs)**

Co(OH)<sub>2</sub> NSs was achieved by mixing CoCl<sub>2</sub> aqueous solution and NaOH aqueous solution. X-ray diffraction (XRD) pattern shows the characteristic diffraction peaks of Co(OH)<sub>2</sub> (JCPDS No. 30-0443), in which the diffraction peaks at 19.0°, 32.4°, 37.9°, 51.4°, and 57.9° can be ascribed to the (001), (100), (101), (102), (110) planes of Co(OH)<sub>2</sub> crystal (Fig. S1 in ESI). Scanning electron microscopy (SEM) image confirms Co(OH)<sub>2</sub> NSs are complete hexagonal nanosheets (Fig. S2A in ESI).

### **Electrochemical measurements**

The electrochemical measurements were carried out using a CHI 660D electrochemical workstation in an H-type electrolytic cell separated by a N117 Nafion membrane at room temperature. The saturated calomel electrode (SCE) is used as the reference electrode, the carbon rod is used as the auxiliary electrode, and the electrocatalyst modified glassy carbon electrode is used as working electrode. 0.5 M Na<sub>2</sub>SO<sub>4</sub> solution (60 mL) is evenly distributed to the cathode and anode compartments. 50 mmol NaNO<sub>3</sub> was added into the cathode compartment for electroreduction of NaNO<sub>3</sub>. All potentials mentioned in the work correspond to the reversible hydrogen electrode potential (RHE), where  $E_{\text{RHE}} = E_{\text{SCE}} + 0.242 \text{ V} + 0.0591\text{pH}$ . The current densities are normalized to the geometric area of the working electrode unless otherwise stated. The catalyst ink was prepared by dispersing 2 mg electrocatalyst in 1 mL of water containing 0.2 mL of isopropyl alcohol and 5  $\mu\text{L}$  Nafion. Then, 4  $\mu\text{L}$  of above suspension was dropped on the surface of the glassy carbon electrode and dry at room temperature.

### **HER activity of CoP NRs and CoP NPs**

HER activity of CoP NRs and CoP NPs were first investigated by linear sweep voltammetry (LSV) technique in 0.5 M Na<sub>2</sub>SO<sub>4</sub> electrolyte. The overpotential values of HER at CoP NRs and CoP NPs are 578 and 652 mV at current density of 10 mA

cm<sup>-2</sup>, respectively (Fig. S8A in ESI). Tafel slope values of HER at CoP NRs and CoP NPs are 97 and 111 mV dec<sup>-1</sup>, respectively, indicating a faster HER kinetics at CoP NRs (Fig. S8B in ESI). These electrochemical results suggest that CoP NRs have higher HER activity than CoP NPs. Indeed, HER activity of CoP NRs and CoP NPs were also investigated in neutral phosphate buffer saline (PBS, pH = 7) electrolyte (Fig. S9 in ESI). The polarization curves display that CoP NRs have still higher HER activity than CoP NPs. The overpotential of HER at CoP NRs is 241 mV at current density of 10 mA cm<sup>-2</sup>, which exceed the HER performance of previously reported CoP nanomaterials in PBS electrolyte (Table S1).

### The Faradaic Efficiency of NO<sub>3</sub><sup>-</sup>-ERR and NH<sub>3</sub> Yield

The chronoamperometry tests of NO<sub>3</sub><sup>-</sup>-ERR were performed at a two-compartment cell with Ar-purged 0.5 M Na<sub>2</sub>SO<sub>4</sub> + 0.05 M NaNO<sub>3</sub> solution and 0.5 M Na<sub>2</sub>SO<sub>4</sub> solution (30 mL in each cell). The faradaic efficiency for NH<sub>4</sub><sup>+</sup> production was defined as charge converted to NH<sub>4</sub><sup>+</sup> divided by the total charge passed through the electrodes during the electrolysis (*Q*), which was calculated according to the following formula:

$$\text{Faradaic efficiency} = \frac{8F \cdot c_{\text{NH}_3} \cdot V}{M_{\text{NH}_3} \cdot Q}$$

The NH<sub>4</sub><sup>+</sup> yield was calculated by following formula:

$$\text{Yield}_{\text{NH}_3} = \frac{c_{\text{NH}_3} \cdot V}{m \cdot t}$$

where  $c_{\text{NH}_3}$  is the mass concentration of NH<sub>3</sub>(aq),  $V$  is the volume of electrolyte in the cathode compartment (30 mL),  $M_{\text{NH}_3}$  is the molar mass of NH<sub>3</sub>,  $t$  is the electrolysis time (3 h),  $F$  is the Faradaic constant (96485 C mol<sup>-1</sup>),  $Q$  is the total charge passing the electrode.  $m$  and  $t$  are the electrocatalyst mass and the reduction reaction time, respectively.

### Determination of ion concentration

The ultraviolet-visible (UV-Vis) spectrophotometer was used to detect the ion concentration of pre- and post-test electrolytes after diluting to appropriate concentration to match the range of calibration curves. The specific detection methods

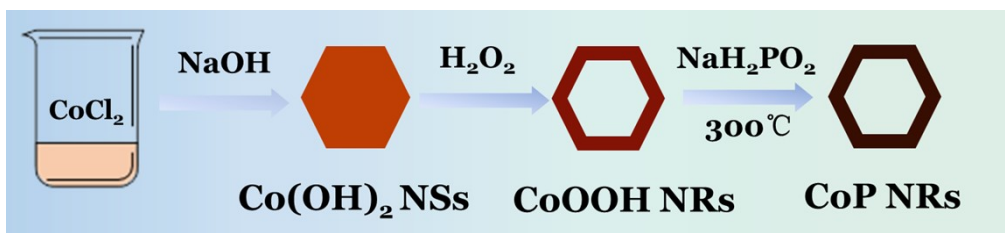
are as follow:

#### **Determination of $\text{NH}_4^+$**

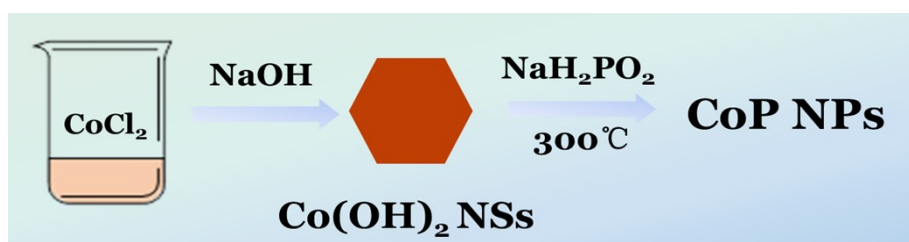
Phenolhypochlorite method was used to detect the  $\text{NH}_3$  concentration. Firstly, the corresponding calibration curve was obtained by UV-vis curves for known concentration of  $\text{NH}_4^+$  in 0.05 M  $\text{Na}_2\text{SO}_4$ . After running chronoamperometry test for 3 h, 1 mL were taken from the electrolyte and put it into the centrifuge tube and diluted to 10 mL with water. Then Stock reagents were added in solution and stand for 3 h. Finally,  $\text{NH}_4^+\text{-N}$  concentration was calculated according to the UV-vis curve and calibration curve.

#### **Determination of nitrite**

A mixture of p-aminobenzenesulfonamide (1.0 g), N-(1-Naphthyl) ethylenediamine dihydrochloride (0.1 g), ultrapure water (100 mL) was used as a color reagent. A certain amount of electrolyte was taken out from the electrolytic cell and diluted to detection range. Next, 0.1 mL color reagent was added into the aforementioned 5 mL solution and mixed uniformly, and the absorption intensity at a wavelength of 542 nm was recorded after sitting for 20 min. The concentration absorbance curve was calibrated using a series of standard sodium nitrite solutions.



Scheme S1. Synthetic procedures of CoP NRs.



Scheme S2. Synthetic procedures of CoP NPs.

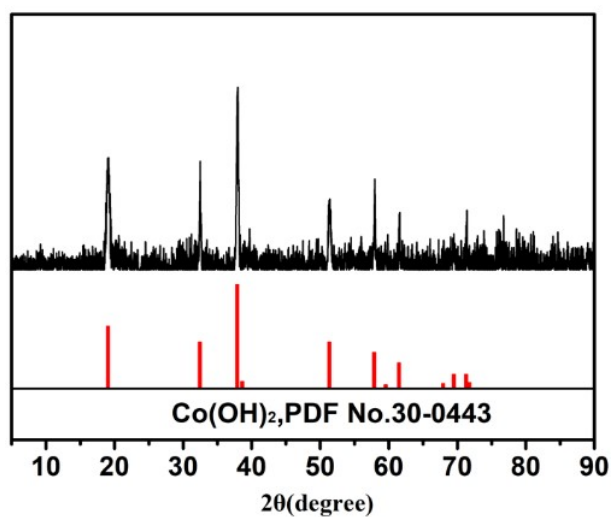


Fig. S1 XRD pattern of  $\text{Co(OH)}_2$  NSs.

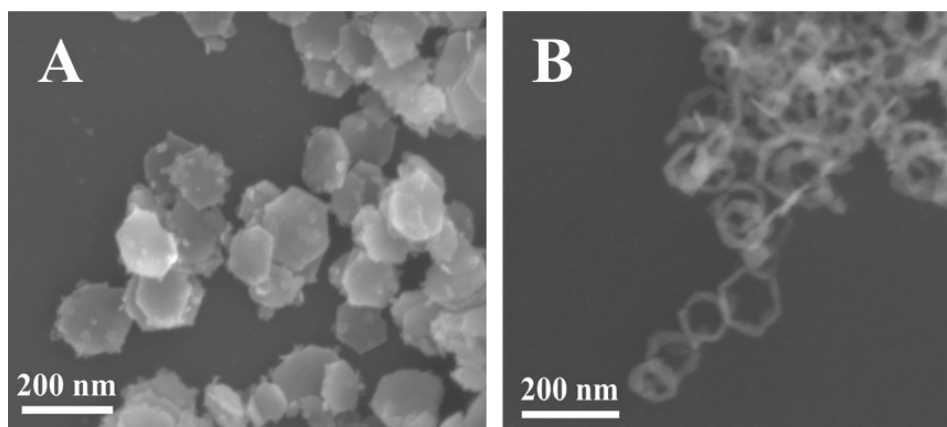


Fig. S2 SEM images of (A)  $\text{Co(OH)}_2$  NSs and (B) CoOOH NRs.

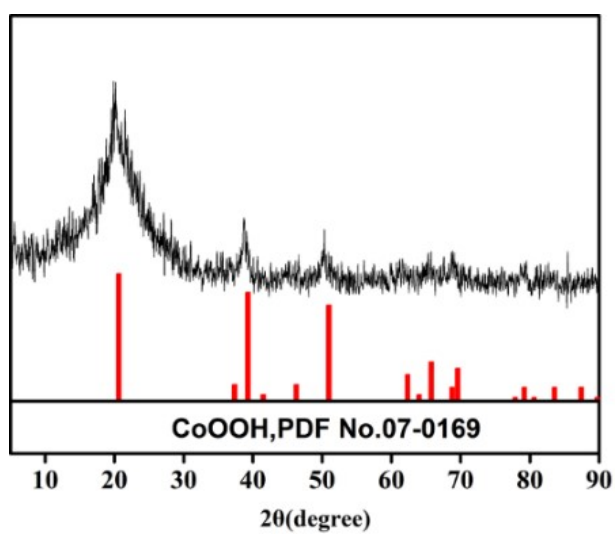


Fig. S3 XRD pattern of CoOOH NRs.

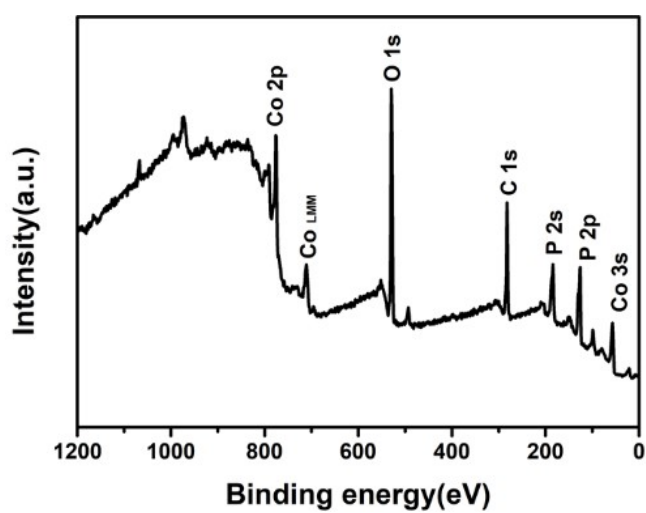
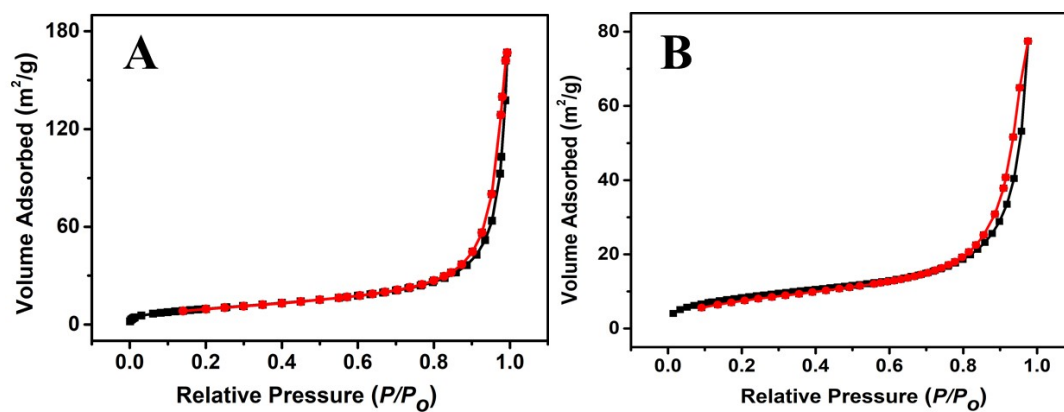
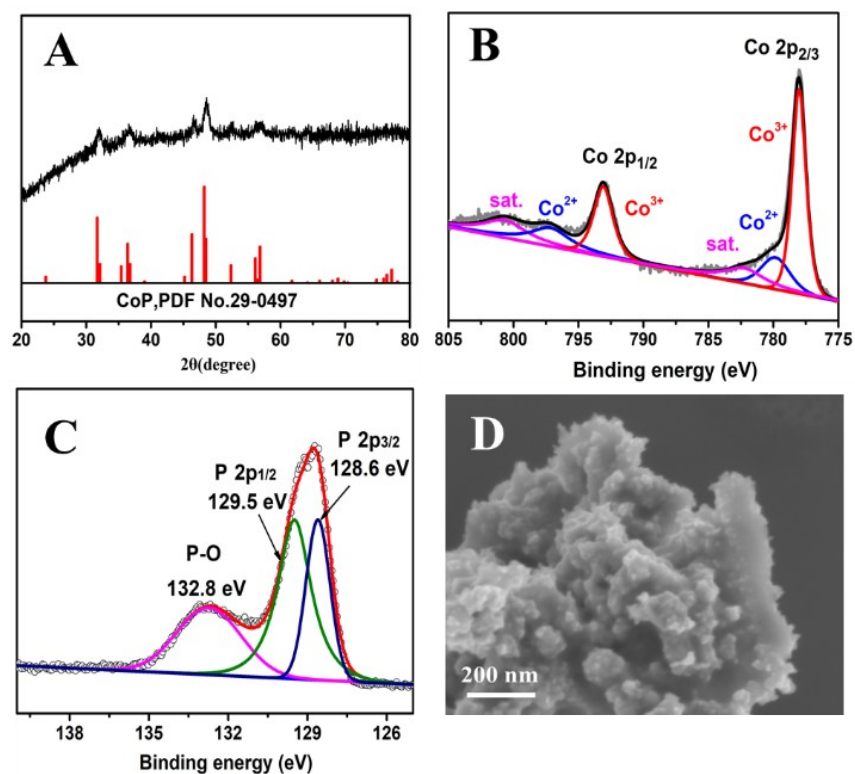


Fig. S4 The survey XPS spectrum of CoP NRs.



**Fig. S5** The nitrogen desorption-adsorption isotherm of (A) CoP NRs and (B) CoP NPs.



**Fig. S6** (A) XRD pattern, (B) Co 2p XPS spectrum, (C) P 2p XPS spectrum, and (D) SEM images of CoP NPs.

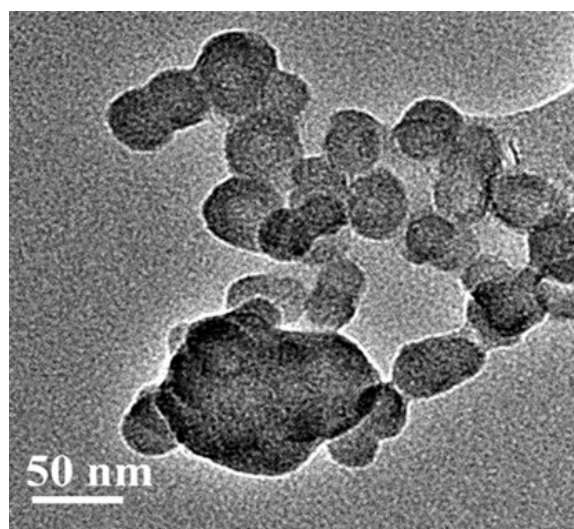


**Fig. S7** TEM images of CoP NPs.

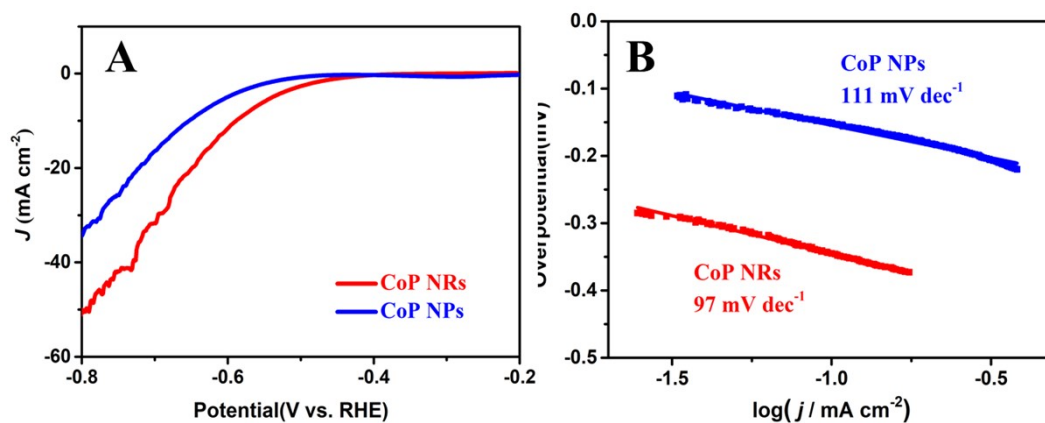


**Fig. S8** (A) LSV curves of CoP NRs and CoP NPs in 0.5 M  $\text{Na}_2\text{SO}_4$  electrolyte at scan rate of  $5 \text{ mV s}^{-1}$  and (B) Tafel plot values of HER at CoP NRs and CoP NPs.

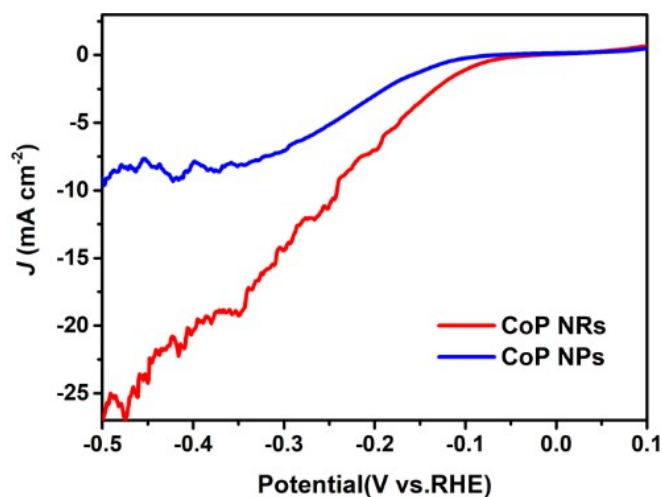


**Fig. S9** (A) LSV curves of CoP NRs and CoP NPs in 1 M PBS solution at  $5 \text{ mV s}^{-1}$ .

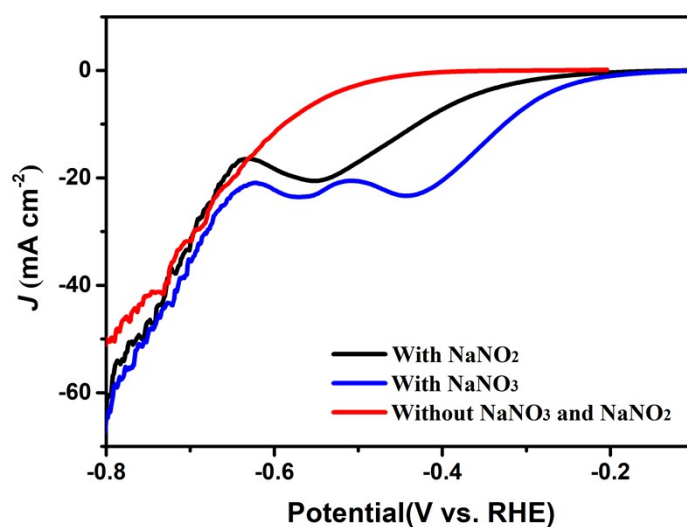


**Fig S10.** LSV curves of CoP NRs in 0.5 M  $\text{Na}_2\text{SO}_4$  solution with and without 50 mM  $\text{NaNO}_3$  or  $\text{NaNO}_2$  at scan rate of  $5 \text{ mV s}^{-1}$ .

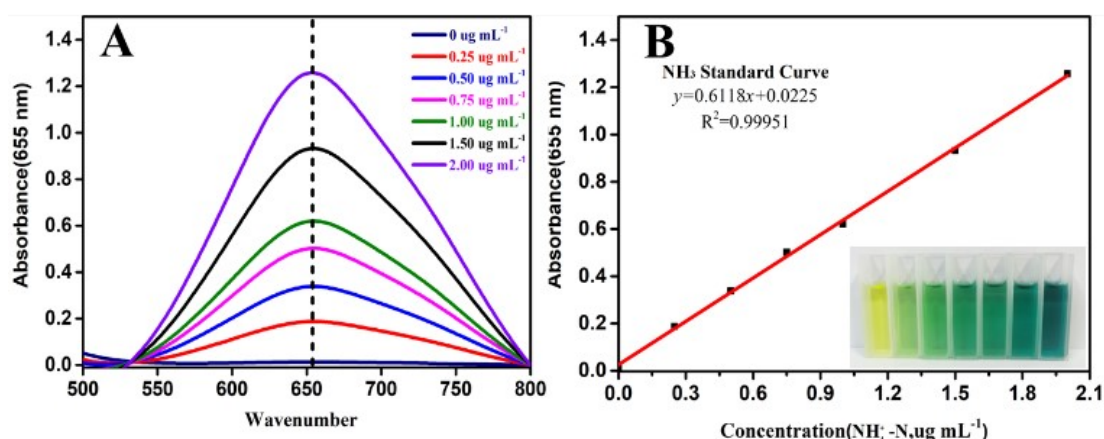


**Fig. S11** Absolute calibration of the phenate method using ammonium solutions of known concentration as standards. (A) UV-vis curves of phenate assays after in darkness for 3 h at room temperature, (B) calibration curve used for estimation of  $\text{NH}_3$  by  $\text{NH}_4^+\text{-N}$  ion concentration. The absorbance at 650 nm was measured by UV-vis spectrophotometer, and the fitting curve shows good linear relation of absorbance with  $\text{NH}_4^+\text{-N}$  concentration ( $y = 0.6118x + 0.0225$ ,  $R^2=0.9995$ ) of three times independent calibration curves.

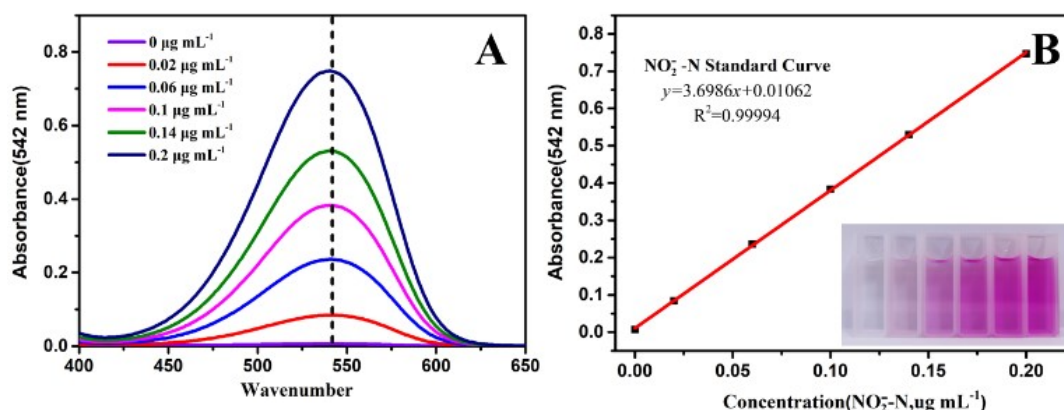


**Fig. S12** The concentration-absorbance curve was calibrated using a series of standard sodium nitrite solutions. (a) UV-vis curves of various  $\text{NO}_2^-$  concentrations after incubated for 10 min at room temperature. (b) Calibration curve used for calculation of  $\text{NO}_2^-$  concentrations. The absorbance at 542 nm was measured by UV-vis spectrophotometer, and the fitting curve shows good linear relation of absorbance with  $\text{NO}_2^-$ -N concentration ( $y = 3.6986x + 0.01062$ ,  $R^2=0.9999$ ) of three times independent calibration curves.

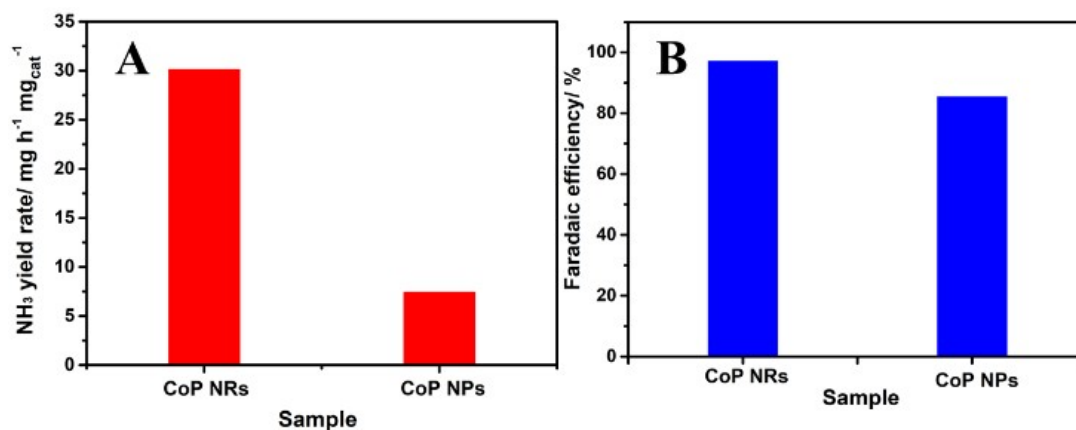


**Fig. S13** (A) NH<sub>3</sub> yield and (B) Faradaic efficiency of NO<sub>3</sub><sup>-</sup>-ERR at CoP NRs and CoP NPs at -0.5 V potential.

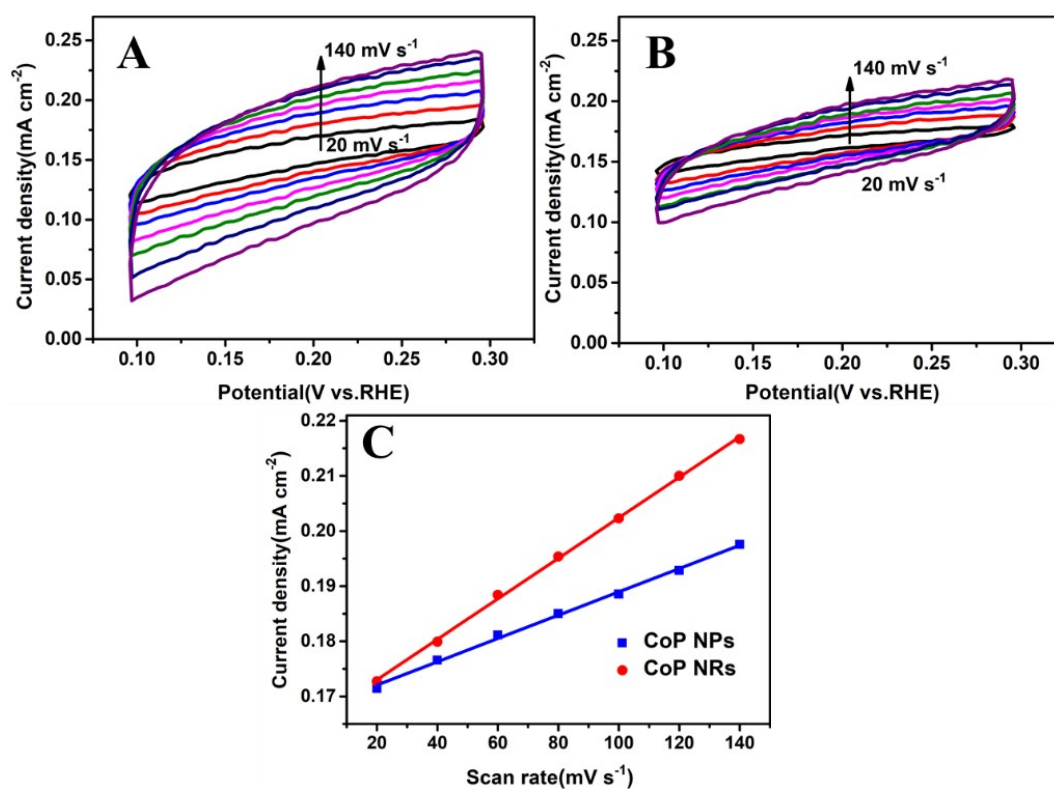


**Fig. S14** CV curves of (A) CoP NRs and (B) CoP NPs in O<sub>2</sub>-saturated 0.5 M Na<sub>2</sub>SO<sub>4</sub> electrolyte at different scan rates. (C) Plots of  $i$  at 0.2 V vs  $v$  at CoP NRs and CoP NPs.

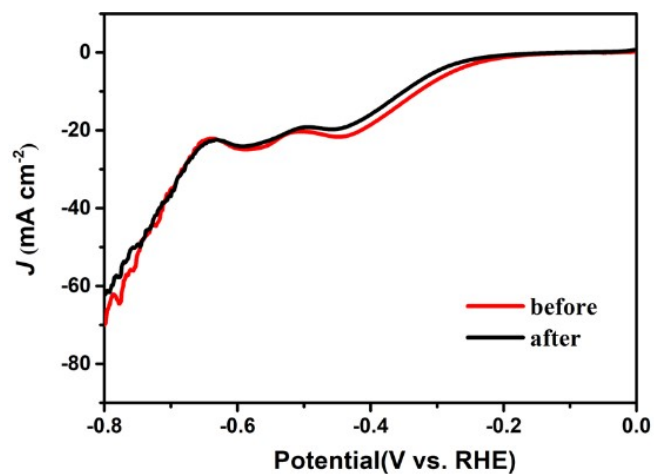


**Fig. S15** LSV curves of CoP NRs in 0.5 M Na<sub>2</sub>SO<sub>4</sub> + 50 mM NaNO<sub>3</sub> electrolyte before and after chronoamperometry measurements.

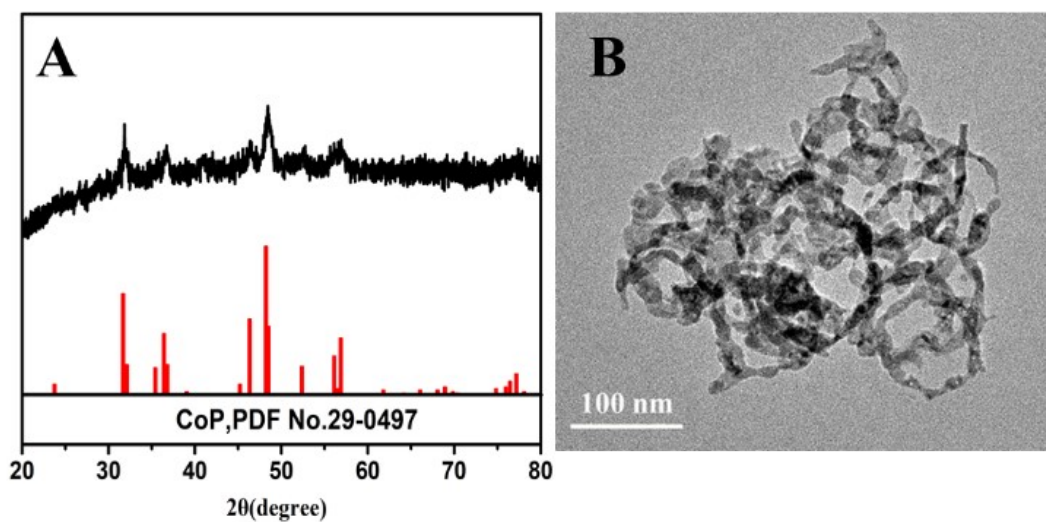


**Fig. S16** (A) XRD pattern and (B) TEM image of CoP NRs after chronoamperometry measurement at same  $-0.5$  V potential.

**Table S1.** HER overpotential at various CoP nanomaterials in 1 M PBS electrolyte.

Catalysts	Electrolyte	$\eta$ value at 10 mA cm <sup>-2</sup>	Ref. (year)
CoP NRs	1.0 M PBS	241 mV	This Work
CoP nanoparticles	1.0 M PBS	~250 mV	2021 <sup>1</sup>
Cobalt phosphosulfide nanosheets	1.0 M PBS	480 mV	2021 <sup>2</sup>
CoP nanosheets	1.0 M PBS	280 mV	2020 <sup>3</sup>
V-doped CoP hollow nanofibers	1.0 M PBS	260 mV	2020 <sup>4</sup>
CoP/Co <sub>2</sub> P nanoparticles in a nitrogen-doped graphitized carbon shell	1.0 M PBS	459 mV	2019 <sup>5</sup>
CoP/NiCoP heterostructure	1.0 M PBS	430 mV	2019 <sup>6</sup>
Ni <sub>1.67</sub> Co <sub>0.33</sub> P/N-doped carbon nanofibers	1.0 M PBS	326 mV	2019 <sup>7</sup>
N-and P-dual-doped core-shell Co <sub>2</sub> P@C nanoparticles	1.0 M PBS	410 mV	2018 <sup>8</sup>
CoP@carbon polyhedron	1.0 M PBS	553 mV	2017 <sup>9</sup>
CoP nanowire	1.0 M PBS	530 mV	2014 <sup>10</sup>

**Table S2.** Faraday efficiency and NH<sub>3</sub> yield of NO<sub>3</sub><sup>-</sup>-ERR at various electrocatalysts.

Catalysts	Electrolyte	Applied potential (vs. RHE)	NH <sub>3</sub> yield (mg h <sup>-1</sup> mg <sup>-1</sup> <sub>cat</sub> )	Faradaic efficiency (%)	Ref. (year)
CoP NRs	0.5 M Na <sub>2</sub> SO <sub>4</sub> + 50 mM NaNO <sub>3</sub>	-0.5 V	30.1	97.1%	This Work
CuPd aerogels	0.5 M K <sub>2</sub> SO <sub>4</sub> + 0.49 mM KNO <sub>3</sub>	-0.46 V	0.784	90.02%	2021 <sup>11</sup>
Fe single atom catalyst	0.50 M KNO <sub>3</sub> +100 mM K <sub>2</sub> SO <sub>4</sub>	-0.66 V	5.245	75%	2021 <sup>12</sup>
Cu nanoplates	0.5 M K <sub>2</sub> SO <sub>4</sub> + 0.49 mM KNO <sub>3</sub>	-0.65 V	0.781	93.26%	2021 <sup>13</sup>
Cu nanowires with concave-convex surface Cu <sub>2+1</sub> O layers	0.5 M K <sub>2</sub> SO <sub>4</sub> + 0.49 mM KNO <sub>3</sub>	-0.55 V	0.576	87.07%	2021 <sup>14</sup>
Cu nano dendrites	0.1 M Na <sub>2</sub> SO <sub>4</sub> +0.1 M NaNO <sub>3</sub>	-0.3 V	0.556	97%	2021 <sup>15</sup>
indium incorporated in sulfur doped graphene	1 M KOH +0.1 M KNO <sub>3</sub>	-0.5 V	12.94	75%	2021 <sup>16</sup>
Pd concave nanocubes	0.1 M NaOH+20 mM NaNO <sub>3</sub>	-0.2 V	0.306	35%	2021 <sup>17</sup>
TiO <sub>2</sub> nanotubes	0.5 M K <sub>2</sub> SO <sub>4</sub> + 0.49 mM KNO <sub>3</sub>	-0.95 V	0.81	85.0%	2020 <sup>18</sup>
Co <sub>3</sub> O <sub>4</sub> @NiO nanotubes	0.5 M K <sub>2</sub> SO <sub>4</sub> +2.35 mM KNO <sub>3</sub>	-0.70 V	0.125	55%	2020 <sup>19</sup>
Ir nanotubes	0.1 M HClO <sub>4</sub> +1 M NaNO <sub>3</sub>	0.06 V	0.921	84.7%	2020 <sup>20</sup>

## References

1. J. Li, J. Wang, F. Jiao, Y. Lin and Y. Gong, *Int. J. Hydrog. Energy*, 2021, **46**, 18353-18363.
2. Y. Hu, Y. Liu, X. Long, Y. Long, F. Li, D. Ma, P. Ma, M. Chen, L. Gao, J. Jin and J. Ma, *J. Power Sources*, 2021, **484**, 229144.
3. L. Yan, B. Zhang, S. Wu and J. Yu, *J. Mater. Chem. A*, 2020, **8**, 14234-14242.

4. R. Zhu, F. Chen, J. Wang, Y. Song, J. Cheng, M. Mao, H. Ma, J. Lu and Y. Cheng, *Nanoscale*, 2020, **12**, 9144-9151.
5. X. Lv, J. Ren, Y. Wang, Y. Liu and Z.-Y. Yuan, *ACS Sustain. Chem. Eng.*, 2019, **7**, 8993-9001.
6. X. Liu, S. Deng, D. Xiao, M. Gong, J. Liang, T. Zhao, T. Shen and D. Wang, *ACS Appl. Mater. Interfaces*, 2019, **11**, 42233-42242.
7. Q. Mo, W. Zhang, L. He, X. Yu and Q. Gao, *Appl. Catal. B*, 2019, **244**, 620-627.
8. Y. Yang, X. Liang, F. Li, S. Li, X. Li, S. P. Ng, C. L. Wu and R. Li, *ChemSusChem*, 2018, **11**, 376-388.
9. H. Tabassum, W. Guo, W. Meng, A. Mahmood, R. Zhao, Q. Wang and R. Zou, *Adv. Energy Mater.*, 2017, **7**(9)
10. J. Tian, Q. Liu, A. M. Asiri and X. Sun, *J. Am. Chem. Soc.*, 2014, **136**, 7587-7590.
11. Y. Xu, K. Ren, T. Ren, M. Wang, M. Liu, Z. Wang, X. Li, L. Wang and H. Wang, *Chem. Commun.*, 2021, **57**, 7525-7528
12. Z. Y. Wu, M. Karamad, X. Yong, Q. Huang, D. A. Cullen, P. Zhu, C. Xia, Q. Xiao, M. Shakouri, F. Y. Chen, J. Y. T. Kim, Y. Xia, K. Heck, Y. Hu, M. S. Wong, Q. Li, I. Gates, S. Siahrostami and H. Wang, *Nat Commun*, 2021, **12**, 2870.
13. Y. Xu, M. Wang, K. Ren, T. Ren, M. Liu, Z. Wang, X. Li, L. Wang and H. Wang, *J. Mater. Chem. A*, 2021, **9**, 16411-16417.
14. T. Ren, K. Ren, M. Wang, M. Liu, Z. Wang, H. Wang, X. Li, L. Wang and Y. Xu, *Chem. Eng. J.* 2021, **426**, 130759.
15. S. B. Patil, T. R. Liu, H. L. Chou, Y. B. Huang, C. C. Chang, Y. C. Chen, Y. S. Lin, H. Li, Y. C. Lee, Y. J. Chang, Y. H. Lai, C. Y. Wen and D. Y. Wang, *J. Phys. Chem. Lett.*, 2021, **2236**, 8121-8128.
16. F. Lei, W. Xu, J. Yu, K. Li, J. Xie, P. Hao, G. Cui and B. Tang, *Chem. Eng. J.*, 2021, **426**, 131317.
17. J. Lim, C.-Y. Liu, J. Park, Y.-H. Liu, T. P. Senftle, S. W. Lee and M. C. Hatzell, *ACS Catal.*, 2021, **11**, 7568-7577.
18. R. Jia, Y. Wang, C. Wang, Y. Ling, Y. Yu and B. Zhang, *ACS Catal.*, 2020, **10**, 3533-3540.
19. Y. Wang, C. Liu, B. Zhang and Y. Yu, *Sci. China Mater.*, 2020, **63**, 2530-2538
20. J.-Y. Zhu, Q. Xue, Y.-Y. Xue, Y. Ding, F.-M. Li, P. Jin, P. Chen and Y. Chen, *ACS Appl. Mater. Interfaces.*, 2020, **12**, 14064-14070.